



HAL
open science

Minimum-Volume Set-Membership State Estimation of LTV Constrained Systems with Sporadic Measurements

Yasmina Becis-Aubry, Nacim Ramdani

► **To cite this version:**

Yasmina Becis-Aubry, Nacim Ramdani. Minimum-Volume Set-Membership State Estimation of LTV Constrained Systems with Sporadic Measurements. 2023 62nd IEEE Conference on Decision and Control (CDC), Dec 2023, Singapore, France. pp.6487-6492, 10.1109/CDC49753.2023.10383257 . hal-04484572

HAL Id: hal-04484572

<https://hal.science/hal-04484572>

Submitted on 24 Apr 2024

HAL is a multi-disciplinary open access archive for the deposit and dissemination of scientific research documents, whether they are published or not. The documents may come from teaching and research institutions in France or abroad, or from public or private research centers.

L'archive ouverte pluridisciplinaire **HAL**, est destinée au dépôt et à la diffusion de documents scientifiques de niveau recherche, publiés ou non, émanant des établissements d'enseignement et de recherche français ou étrangers, des laboratoires publics ou privés.

Minimum-volume set-membership state estimation of LTV constrained systems with sporadic measurements

Yasmina BECIS-AUBRY and Nacim RAMDANI

Abstract—This paper presents a recursive ellipsoidal set-membership state estimation algorithm for discrete-time linear time-varying (LTV) models with additive bounded disturbances affecting state evolution and sporadic measurement equations. The state vector is subject to linear equality and/or inequality constraints, which are mathematically viewed as additional measurements. A novel approach is developed considering the unprecedented fact that, owing to equality constraints, the ellipsoid characterizing all possible values of the state vector has a zero volume and its shape matrix is non invertible. A new size criterion, the pseudo-volume, is introduced and minimized in both the prediction and correction phases.

I. INTRODUCTION

Many physical systems are subject to equality constraints (e.g. target tracking, 2D restrictions in 3D motion, fixed speed for a robotic arm) or state space inequality constraints (e.g. motors maximum speed), owing to relevant physical laws, geometric considerations, and kinematic limits. Nonetheless, constrained classical state estimation, such as the Kalman Filtering (KF), has historically attracted limited interest, [1], [2], most likely because of challenging modeling limitations and increased computational costs. And interestingly, there are even fewer constrained problems, when it comes to set-membership state estimation (explained below). As a result, (in)equality constraints are frequently ignored in typical state estimation applications. However, taking into account such constraints has a significant impact on the estimation process (the constrained estimate may differ significantly from the unconstrained one) and consequentially reduces the state bounding set (roughly viewed as the confidence region) by projecting it onto a state subspace of lower dimension.

Set-membership estimation approaches differ from classical (stochastic) methods (such as the KF) in the fact that the stochastic information on the disturbances and the initial estimate, in the former, are replaced by sets, *i.e.*, known bounds, in the latter and instead of the point-wise estimate, we have a bounding set. This bounding set can have different shapes. Four main set characterizations share research interests in set-membership state estimation: those using intervals or boxes (balls for the ∞ -norm), parallelotopes (affine injective or bijective maps of boxes), zonotopes (surjective affine maps of boxes) and ellipsoids (affine maps

of balls for the 2-norm). The techniques using zonotopes are more precise than those using ellipsoids, as stated in the comparative review of set-membership approaches (because the complexity of the ellipsoid is fixed by the dimension of the state to estimate, while the complexity of the zonotope is flexible according to the chosen accuracy). But it was also mentioned that the ellipsoidal methods have lower computational complexity. The use of zonotopes involves costly convex optimization problems, which, in the case of LTV systems, should be solved at each step during real-time operation (the review covered only linear time-invariant models). Furthermore, the volume of the state bounding set appears to be the most meaningful, but at the same time, the most computationally expensive cost function to be minimized, which involves solving an optimization problem when using zonotopes. Therefore, the volume optimization criterion was not included in the above-mentioned study.

Our goal in this note is to demonstrate that, even for time-varying systems (which require online computations), volume minimization can be completely undemanding when using ellipsoidal bounding sets for state characterization, and that equality and inequality constraints are not more computationally expensive than conventional bounded noise measurements. In order to address the challenging issue of the equality constraints, a new concept of pseudo-volume is introduced, leading to a number of new results.

The remainder of this paper is organized as follows. After this introduction, which is completed with some notations and definitions, the second section recaptures the constrained set membership state estimation problem with sporadic measurements. The third section deals with the time prediction stage, and the measurement correction stage of the estimation algorithm is detailed in the forth section. The pseudo-volumes of the predicted and corrected ellipsoids were minimized in both steps. Some aspects of the convergence are addressed in the fifth section. The sixth section of this paper presents some numerical simulations, and the paper is briefly concluded in the seventh section.

A. Notations and definitions

1. $\mathbb{R} :=] - \infty, +\infty[$ and $\mathbb{R}_+^* :=]0, +\infty[$; $\mathbb{N} = \{0, 1, 2, \dots\}$, $\mathbb{N}^* = \mathbb{N} - \{0\}$. Lowercase letters are used for scalars, uppercase ones for matrices, bold lowercase ones for vectors and calligraphic capital ones for sets.
2. $\mathbf{a} := [a_1 \dots a_n]^T \in \mathbb{R}^n$ (bold) and $A := [a_j]_{j=1}^m \in \mathbb{R}^{n \times m}$.
3. $\mathbf{0}_n \in \mathbb{R}^n$, $\mathbf{0}_{n,m} \in \mathbb{R}^{n \times m}$ are vector and matrix of zeros.

This project has received funding from the European Union's Horizon 2020 research and innovation programme under the Marie Skłodowska-Curie grant agreement No 101007673.

*The authors are with Univ. Orléans, INSA CVL, PRISME EA 4229, F45072 Orléans, FRANCE. Yasmina.Becis@univ-orleans.fr.

4. A^T , A^{-1} , A^\dagger , $\text{rank}(A)$, $\mathcal{N}(A)$, $\mathcal{R}(A)$, and $|A|$ are *resp.* the transpose, inverse, pseudoinverse, rank, kernel, range, and determinant of A .
5. The matrix $M \in \mathbb{R}^{n \times n}$ is SPD (SPSD) *i.e.* Symmetric Positive (Semi-) Definite, if and only if $\forall \mathbf{x} \in \mathbb{R}^n - \{\mathbf{0}_n\}$, $\mathbf{x}^T M \mathbf{x} > 0$ (*resp.* $\mathbf{x}^T M \mathbf{x} \geq 0$).
6. $\|\mathbf{x}\| := \|\mathbf{x}\|_2 = \sqrt{\mathbf{x}^T \mathbf{x}}$; $\|\mathbf{x}\|_\infty := \max_{1 \leq i \leq n} |x_i|$.
7. $\mathcal{B}_2^n := \{\mathbf{z} \in \mathbb{R}^n \mid \|\mathbf{z}\|_2 \leq 1\}$ and $\mathcal{B}_\infty^n := [-1, 1]^n$ are unit balls in \mathbb{R}^n : centered unit hypersphere and hypercube *resp.*
8. $\mathcal{S}_1 \oplus \mathcal{S}_2 := \{\mathbf{x} \in \mathbb{R}^n \mid \mathbf{x} = \mathbf{x}_1 + \mathbf{x}_2, \mathbf{x}_1 \in \mathcal{S}_1, \mathbf{x}_2 \in \mathcal{S}_2\}$.
9. $\mathcal{E}(\mathbf{c}, P) := \{\mathbf{x} \in \mathbb{R}^n \mid \mathbf{x} = \mathbf{c} + M\mathbf{z}, \mathbf{z} \in \mathcal{B}_2^n, P = MM^T\}$ is an ellipsoid in \mathbb{R}^n . If P is SPD, then we have also $\mathcal{E}(\mathbf{c}, P) := \{\mathbf{x} \in \mathbb{R}^n \mid (\mathbf{x} - \mathbf{c})^T P^{-1} (\mathbf{x} - \mathbf{c}) \leq 1\}$.
10. $\mathcal{Z}(\mathbf{c}, L) := \{\mathbf{x} \in \mathbb{R}^n \mid \mathbf{x} = \mathbf{c} + L\mathbf{z}, \mathbf{z} \in \mathcal{B}_\infty^m\}$ a zonotope.

II. PROBLEM FORMULATION

Consider the following discrete time, LTV system:

$$\mathbf{x}_k = A_{k-1} \mathbf{x}_{k-1} + B_{k-1} \boldsymbol{\tau}_{k-1} + R_{k-1} \mathbf{w}_{k-1}, \quad (1a)$$

where $\mathbf{x}_0 \in \mathcal{E}(\hat{\mathbf{x}}_0, \varsigma_0 P_0) =: \mathcal{E}_0 \subset \mathbb{R}^n$ and $\mathbf{w}_k \in \mathcal{B}_\infty^{m_k}$, (1b) $k \in \mathbb{N}^*$ is the time step, $\mathbf{x}_k \in \mathbb{R}^n$ is the unknown state vector to be estimated, $\boldsymbol{\tau}_k \in \mathbb{R}^l$ is a known control vector and $\mathbf{w}_k \in \mathbb{R}^{m_k}$ is an unobservable bounded process noise vector with unknown statistical characteristics and its size $m := m_k$ is possibly time varying¹. \mathcal{E}_0 is a known ellipsoid, of center $\hat{\mathbf{x}}_0$ (the initial estimate of \mathbf{x}_k) and of shape matrix $\varsigma_0 P_0$ (P_0 is an SPD matrix, ς_0 is a scaling positive scalar which can be set to 1). $A_k \in \mathbb{R}^{n \times n}$ and $B_k \in \mathbb{R}^{n \times l}$ are known state and input matrices, *resp.* and $R_k \in \mathbb{R}^{n \times m}$ is the generator matrix that defines the zonotope bounding the unknown input vector $R_k \mathbf{w}_k \in \mathcal{Z}(\mathbf{0}_n, R_k)$. Now, we consider the following inequalities that represent the observations of the system (1):

$$y_{k_i} \leq \mathbf{f}_{k_i}^T \mathbf{x}_k \leq \bar{y}_{k_i}, \quad i \in \{1, \dots, p_k\} = \mathcal{D}_k \cup \mathcal{G}_k \cup \mathcal{H}_k, \quad (2a)$$

defining a polyhedral constraint on the state vector, $\mathcal{P}_k \ni \mathbf{x}_k$, formed by:

- **Intersecting strips (for $i \in \mathcal{D}_k$):** y_{k_i} and \bar{y}_{k_i} are both available: $-\infty < y_{k_i} < \bar{y}_{k_i} < +\infty$. For such an i , (2a) represents a typical *measurement with a bounded noise*.
- **Halfspaces (for $i \in \mathcal{G}_k$):** only one bound, either y_{k_i} or \bar{y}_{k_i} , is available ($\bar{y}_{k_i} = +\infty$ or $y_{k_i} = -\infty$, *resp.*). For such an i , (2a) models a linear *inequality constraint on the state vector*.
- **Hyperplanes (for $i \in \mathcal{H}_k$):** both bounds are equal $y_{k_i} = \bar{y}_{k_i}$. For such an i , (2a) represents a linear *equality constraint on the state vector*.

The observation matrix $F_k := [\mathbf{f}_{k_j}]_{j=1}^{p_k} \in \mathbb{R}^{n \times p_k}$ is time varying as is the number of its columns, $p := p_k \in \mathbb{N}$, which¹ can sometimes be zero (in the absence of measurements). Indeed, the measurements are available in varying amounts, at not all but some sporadic time steps $k \in \mathcal{K}$:

$$\mathcal{K} := \{k \in \mathbb{N} \mid p_k \neq 0\}. \quad (2b)$$

¹All variables defined from now on are time varying but the subscript k will be skipped on some of them for an improved readability.

Note that the typical output equation

$$\mathbf{y}_k = F_k^T \mathbf{x}_k + D_k \mathbf{v}_k, \quad \mathbf{v}_k \in \mathcal{B}_\infty^{p_k} \quad (2c)$$

is a particular case of (2a), where $y_{k_i} = \frac{\bar{y}_{k_i} + y_{k_i}}{2}$ and D_k is a diagonal matrix with $d_{ii} = \frac{\bar{y}_{k_i} - y_{k_i}}{2}$, $i \in \{1, \dots, p_k\}$. However, (2c) is limited to cases where both bounds \bar{y}_{k_i} and y_{k_i} are known and finite, *i.e.*, $i \in \mathcal{D}_k \cup \mathcal{H}_k$ and cannot represent the inequality constraints on the state vector, where either \bar{y}_{k_i} or y_{k_i} is unavailable ($i \in \mathcal{G}_k$).

First, we aim to quantify, at each time step k , the “optimal” set containing all possible occurrences of the state vector and then express the conditions of convergence of such a set. Let $\mathcal{E}_k := \mathcal{E}(\hat{\mathbf{x}}_k, \varsigma_k P_k)$ be the ellipsoid containing all possible values of the true state vector \mathbf{x}_k . As the matrix P_k is decreasing² during the measurement correction stage, it should be noted that the parameter ς_k is used to model the possibly non-monotonic part of the ellipsoid shape matrix \mathcal{E}_k . It can be viewed as the upper bound of a squared weighted estimation error norm, $(\mathbf{x}_k - \hat{\mathbf{x}}_k)^T P_k^{-1} (\mathbf{x}_k - \hat{\mathbf{x}}_k)$. The progression law for the ellipsoid \mathcal{E}_k is established in the following while a chosen size criterion is optimized.

III. TIME PREDICTION STAGE

In the first paragraphs of this section, important tools are established in view of the development of an optimal prediction algorithm in § III-B. This tools represent the first main contribution of this paper.

A. Minimal pseudo-volume predicted ellipsoid

The following lemma gives the parameterized family of ellipsoids $\mathcal{E}_\oplus(\mu)$, which contains the Minkowski sum of the ellipsoid $A\mathcal{E}(\mathbf{c}, \varsigma P) := \{A\mathbf{x} \mid \mathbf{x} \in \mathcal{E}(\mathbf{c}, \varsigma P)\}$ and the line segment $\mathcal{Z}(\mathbf{0}_n, \mathbf{r}) = \mathcal{E}(\mathbf{0}_n, \mathbf{r}\mathbf{r}^T)$.

Lemma 3.1 ([3]): Let $\mathbf{c}, \mathbf{u}, \mathbf{r} \in \mathbb{R}^n - \{\mathbf{0}_n\}$, $A \in \mathbb{R}^{n \times n}$ and $P \in \mathbb{R}^{n \times n}$ SPD. then

$$A\mathcal{E}(\mathbf{c}, \varsigma P) \oplus \mathcal{Z}(\mathbf{u}, \mathbf{r}) \subset \mathcal{E}_\oplus(\mu) := \mathcal{E}(\mathbf{c}_\oplus, \varsigma P_\oplus(\mu)), \quad \text{where} \quad (3a)$$

$$\mathbf{c}_\oplus := A\mathbf{c} + \mathbf{u},$$

$$P_\oplus(\mu) := (1 + \mu)Q + \frac{1+\mu}{\varsigma\mu} \mathbf{r}\mathbf{r}^T, \quad \text{with } Q := APA^T. \quad (3b)$$

In the next paragraph, the positive scalar parameter μ is chosen so that the size of $\mathcal{E}_\oplus(\mu)$ is minimized.

1) *Pseudo-volume:* The volume, one of the most meaningful measures of a bounded set’s size, is minimized. Since the eigenvalues of $\varsigma P_\oplus(\mu)$ are the squared semi-axes lengths of $\mathcal{E}_\oplus(\mu)$, the (squared) volume is proportional to their product, *i.e.*, to $|\varsigma P_\oplus(\mu)|$. As explained in § IV, every equality constraint on the state vector, modeled by a measurement $i \in \mathcal{H}_k$, is very likely to cause the ellipsoid shape matrix P_k to lose rank by one during the correction stage. This results in zero axes lengths and therefore a zero volume of \mathcal{E}_k . We will then introduce a generalized volume, the *pseudo-volume* of an ellipsoid, whose usual volume can be zero.

First, note that when $P \in \mathbb{R}^{n \times n}$ is SPD, the usual volume of an ellipsoid, $\text{vol}(\cdot)$, is: $\text{vol}(\mathcal{E}(\mathbf{c}, P)) =: \text{vol}(\mathcal{B}_2^n) \sqrt{|P|}$,

where $\text{vol}(\mathcal{B}_2^n) := \frac{\pi^{\frac{n}{2}}}{\Gamma(\frac{n}{2} + 1)}$, [4], where Γ is the Euler Gamma-function.

²A SPD matrix P_k is said to be decreasing if $P_{k-1} - P_k$ is PSD.

Definition 3.1: For any SPSD matrix P and any $\mathbf{c} \in \mathbb{R}^n$, the SPV (squared pseudo-volume) of the ellipsoid $\mathcal{E}(\mathbf{c}, P)$ is

$$\text{spv}(\mathcal{E}(\mathbf{c}, P)) =: \text{vol}^2(\mathcal{B}_2^q) |P|_{\dagger},$$

where $q := \text{rank}(P)$ and $|P|_{\dagger} =: \lim_{t \rightarrow 0} \frac{|P+tI_n|}{t^{n-q}}$ is the pseudo-determinant of P (the product of all its nonzero eigenvalues). The pseudo-volume of $\mathcal{E}(\mathbf{c}, P)$ is nothing but the volume of the orthogonal projection of $\mathcal{E}(\mathbf{c}, P)$ onto $\mathcal{R}(P)$.

2) *Optimal value of the parameter μ and one-rank updates:* The rank and pseudo-determinant expressions of the ellipsoid's SPSD shape matrix, prior to its minimization, are provided in the following result, as one-rank update expressions.

Proposition 3.2: $\forall Q \in \mathbb{R}^{n \times n}$ SPSD, $\forall \mathbf{r} \in \mathbb{R}^n, \forall a, b \in \mathbb{R}_+^*$, if $Q_+ := b(Q + \text{arr}^T)$, then

$$i. \text{rank}(Q_+) =: q_+ = \begin{cases} q := \text{rank}(Q), & \text{if } \mathbf{v} = \mathbf{0}_n, \\ q + 1, & \text{otherwise.} \end{cases} \quad (4a)$$

$$ii. |Q_+|_{\dagger} = \begin{cases} b^q |Q|_{\dagger} (1 + \text{arr}^T \mathbf{u}), & \text{if } \mathbf{v} = \mathbf{0}_n; \\ b^{q+1} |Q|_{\dagger} a \mathbf{v}^T \mathbf{v}, & \text{otherwise;} \end{cases} \quad (4b)$$

$$\text{where } \mathbf{u} := Q^{\dagger} \mathbf{r} \text{ and } \mathbf{v} := (I_n - QQ^{\dagger}) \mathbf{r}. \quad (4c)$$

Proof. cf. Appendix A.2 in [5]. \square

Theorem 3.3: $\mathcal{E}_{\oplus}(\mu)$, defined in (3), has the minimum pseudo-volume if $\mu = \mu^* := \arg \min_{\mu \in \mathbb{R}_+^*} |P_{\oplus}(\mu)|_{\dagger}$:

$$\mu^* = \begin{cases} \frac{1}{2q} \sqrt{(q-1)^2 h^2 + 4qh} - \frac{q-1}{2q} h, & \text{if } \mathbf{v} = \mathbf{0}_n, \\ \frac{1}{q}, & \text{otherwise;} \end{cases} \quad (5a)$$

$$\mathbf{u}, \mathbf{v} \text{ given in (4c), } q := \text{rank}(Q) \text{ and } h := \zeta^{-1} \mathbf{r}^T \mathbf{u}. \quad (5b)$$

Proof. cf. Appendix A.3 in [5]. \square

It is important to note that minimizing the volume of $\mathcal{E}_{\oplus}(\mu)$ requires the pseudoinverse of the matrix P . In the following proposition, we present the one-rank update of the pseudoinverse of an ellipsoid's shape matrix, allowing to derived it recursively.

Proposition 3.4: If $Q_+ := b(Q + \text{arr}^T)$, then

$$Q_+^{\dagger} = \frac{1}{b} (Q^{\dagger} + \Delta), \text{ where} \quad (6a)$$

$$\Delta := \begin{cases} \frac{1}{\|\mathbf{r}\|^2} \left(\frac{c}{\|\mathbf{r}\|^2} \mathbf{v} \mathbf{v}^T - \mathbf{u} \mathbf{v}^T - \mathbf{v} \mathbf{u}^T \right), & \text{if } \mathbf{v} \neq \mathbf{0}_n; \\ -\frac{1}{c} \mathbf{u} \mathbf{u}^T, & \text{otherwise.} \end{cases} \quad (6b)$$

where $c := \frac{1 + \text{arr}^T Q^{\dagger} \mathbf{r}}{a}$ and \mathbf{u} and \mathbf{v} are defined in (4c).

Proof. Obtained by using Thm 1 and Thm 3 of [6]. \square

B. The time prediction algorithm

Let $\mathcal{E}_{k+1/k}$ be the superset of the ‘‘reachable set’’ of every possible value of $\mathbf{x}_k \in \mathcal{E}_k$ evolving according to the plant dynamics eq. (1a) and subject to (1b). The parameterized (by μ) family of the ellipsoids $\mathcal{E}_{k+1/k}$ that contain $A_k \mathcal{E}_k \oplus \mathcal{Z}(\mathbf{0}_n, R_k)$ is given in the following theorem.

Theorem 3.5 ([3]): If $\mathbf{x}_k \in \mathcal{E}_k$, obeying to (1), then $\forall \mu_i \in \mathbb{R}_+^*, \forall i \in \{1, \dots, m\}, \mathbf{x}_{k+1} \in \mathcal{E}_{k+1/k_m}$, where

$$\mathcal{E}_{k+1/k_i} := \mathcal{E}(\hat{\mathbf{x}}_{k+1/k_i}, \varsigma_k Q_i) \supseteq \mathcal{E}_{k+1/k_{i-1}} \oplus \mathcal{Z}(\mathbf{0}_n, \mathbf{r}_{k_i}), \quad (7a)$$

$$\hat{\mathbf{x}}_{k+1/k} := A_k \hat{\mathbf{x}}_k + B_k \boldsymbol{\tau}_k, \quad (7a)$$

$$Q_i := (1 + \mu_i) \left(Q_{i-1} + \frac{1}{\mu_i \varsigma_k} \mathbf{r}_{k_i} \mathbf{r}_{k_i}^T \right), \quad (7b)$$

$$Q_0 := A_k P_k A_k^T; \quad (7c)$$

where \mathbf{r}_{k_i} is the i^{th} column of R_k .

Proof. cf. Appendix A.4 in [5] (Thm 3.6). \square

Given the ellipsoid \mathcal{E}_k at the time step k , Thm 3.5 provides the predicted ellipsoid $\mathcal{E}_{k+1/k} := \mathcal{E}(\hat{\mathbf{x}}_{k+1/k}, \varsigma_k P_{k+1/k})$ whose center is computed as in (7a) and whose shape matrix (up to the factor ς_k), $P_{k+1/k} := Q_m$, is given, by the recursive formula (7b)-(7c), which depends on μ_i , for $i \in \{1, \dots, m\}$. Now, the results of § III-A.1 are employed in order to express on one hand, the optimal value, $\mu^* := \arg \min_{\mu_i \in \mathbb{R}_+^*} |Q_i|_{\dagger}$, that minimizes the pseudo-volume of \mathcal{E}_{k+1/k_i} ; and on the other hand, the recursive formulas of the pseudoinverse and the rank of $P_{k+1/k}$, needed for the computation of μ^* .

Theorem 3.6: \mathcal{E}_{k+1/k_i} (cf. Thm 3.5) has the minimum pseudo-volume if $\mu_i = \mu^*$, given by (5a), where

$$q := \kappa_{i-1}, \quad h := \varsigma_{k_i}^{-1} \mathbf{r}_{k_i}^T \mathbf{u}, \quad (8a)$$

$$\mathbf{u} := \Theta_{i-1} \mathbf{r}_{k_i}, \quad \mathbf{v} := \mathbf{r}_{k_i} - Q_{i-1} \mathbf{u}, \quad (8b)$$

$$\kappa_i := \begin{cases} \kappa_{i-1}, & \text{if } \mathbf{v} = \mathbf{0}_n, \\ \kappa_{i-1} + 1 & \text{otherwise } (\kappa_i = \text{rank}(Q_i)); \end{cases} \quad (8c)$$

$$\kappa_0 := \begin{cases} q_k & \text{if } \text{rank}(A_k) = n; \\ \text{rank}(Q_0), & \text{otherwise;} \end{cases} \quad (8d)$$

$$\text{where } q_k := \text{rank}(P_k) \text{ (cf. (12f)) and } q_{k+1/k} := \kappa_m, \quad (8e)$$

$$\Theta_i := \frac{1}{1 + \mu_i} (\Theta_{i-1} + \Delta_i), \quad i \in \{1, \dots, m\} \quad (\Theta_i := Q_i^{\dagger}), \quad (8f)$$

$$\Theta_0 := Q_0^{\dagger} = (A_k P_k A_k^T)^{\dagger}, \quad (8g)$$

$$\Delta_i := \Delta \text{ is given by (6b),} \quad (8h)$$

where $\mathbf{r} := \mathbf{r}_{k_i}$ and $c := \varsigma_k \mu_i + \mathbf{r}_{k_i}^T \mathbf{u}$.

Proof. Direct consequence of Thm 3.3 and Prop. 3.4 where $a := \frac{1}{\mu_i \varsigma_k}$ and $b := 1 + \mu_i$. \square

Algorithm 1 reproduces Thms 3.5, 3.6 that compute $\mathcal{E}_{k+1/k}$ from \mathcal{E}_k .

Algorithm 1 Minimal pseudo-volume predicted ellipsoid

Input: $\mathbf{x}, P, \varsigma, q, A, B, \mathbf{r}_1 \dots \mathbf{r}_m, \boldsymbol{\tau}, m$

Output: \mathbf{x}, P, q

- 1: $Q := A P A^T$ {cf. (7c)};
 - 2: $\Theta := Q^{\dagger}$ {cf. (8g)};
 - 3: $q := \text{rank}(Q)$ {skipped if $\text{rank}(A_k) = n$ cf. (8d)};
 - 4: **for** $i = 1, \dots, m$ **do**
 - 5: $\mathbf{u} := \Theta \mathbf{r}_i; \mathbf{v} := \mathbf{r}_i - Q \mathbf{u}$ {cf. (8b)};
 - 6: **if** $\mathbf{v} = \mathbf{0}_n$ **then**
 - 7: $h := \varsigma \mathbf{r}_i^T \mathbf{u}$ {cf. (8a)};
 - 8: $\mu = \frac{1}{2q} \sqrt{(q-1)^2 h^2 + 4qh} - \frac{q-1}{2q} h$ {cf. (5a)};
 - 9: $\Delta := -\frac{1}{\varsigma \mu + \mathbf{r}_i^T \mathbf{u}} \mathbf{u} \mathbf{u}^T$ {cf. (8h) and (6b)};
 - 10: **else**
 - 11: $\mu = \frac{1}{q}$ {cf. (5a)}; $q \leftarrow q + 1$ {cf. (8c)};
 - 12: $V := \mathbf{u} \mathbf{v}^T$;
 - 13: $\Delta := \frac{1}{\|\mathbf{r}_i\|^2} \left(\frac{\varsigma \mu + \mathbf{r}_i^T \mathbf{u}}{\|\mathbf{r}_i\|^2} \mathbf{v} \mathbf{v}^T - V - V^T \right)$ {cf. (8h)};
 - 14: **end if**
 - 15: $Q \leftarrow (1 + \mu)(Q + \frac{1}{\mu \varsigma} \mathbf{r}_i \mathbf{r}_i^T)$ {cf. (7b)};
 - 16: $\Theta \leftarrow (1 + \mu)^{-1} (\Theta + \Delta)$ {cf. (8g)};
 - 17: **end for**
 - 18: $\mathbf{x} \leftarrow A \mathbf{x} + B \boldsymbol{\tau}$ {cf. (7a)}; $P \leftarrow Q$
-

IV. MEASUREMENT CORRECTION STAGE

The predicted ellipsoid $\mathcal{E}_{k/k-1}$ taking into account the measurements up to time step $k-1$, if any, is now intersected with the polyhedron \mathcal{P}_k , defined in (2). This is achieved by successively intersecting $\mathcal{E}_{k/k-1}$ with the sets defined by (2a), for each $i \in \{1, \dots, p\}$.

The correction stage allows to find $\mathcal{E}_k \supset \mathcal{S}_k$, where

$$\mathcal{S}_k := \mathcal{E}_{k/k-1} \cap \mathcal{P}_k. \quad (9)$$

It is important to note that the intersection of a n -dimensional ellipsoid \mathcal{E} , of a q -rank shape matrix P , with an intersecting (non parallel and non containing³) hyperplane \mathcal{H} results in a flattened, *i.e.*, having some zero-length axes, n -dimensional ellipsoid with a shape matrix of rank $q-1$. And the good news is that there is no need to circumscribe it by another ellipsoid, as would be the case when cutting with a strip or a halfspace, since the class of ellipsoids is the only one, among the zonotopes, parallelotopes and intervals, that is closed under the intersection with hyperplanes.

Now, parts of Thms 4.1, 4.2 and 4.4 of [3], which express the ellipsoid that bounds the intersection of an ellipsoid with a halfspace, a strip and hyperplane, *resp.* are summarized in the following theorem.

Theorem 4.1 ([3]): Let $\mathbf{c} \in \mathbb{R}^n$, $\varsigma \in \mathbb{R}_+^*$, $\underline{y} \leq \bar{y} \in \mathbb{R}$, $P \in \mathbb{R}^{n \times n}$ SPSD, $\mathbf{f} \in \mathbb{R}^n - \{\mathbf{0}_n\}$ and let $\mathbf{x} \in \mathcal{E} := \mathcal{E}(\mathbf{c}, \varsigma P)$. If $\underline{y} \leq \mathbf{f}^T \mathbf{x} \leq \bar{y}$, where $\underline{y} \neq \bar{y}$ (either \underline{y} or \bar{y} can be infinite) and if $-\rho < \bar{y} < \bar{\rho}$ or $-\rho < \underline{y} < \bar{\rho}$, then $\forall \beta \in]0, 1[$,

$$\mathbf{x} \in \mathcal{E}_\cap(\beta) := \mathcal{E}(\mathbf{c}_\cap(\beta), \varsigma_\cap(\beta) P_\cap(\beta)), \quad \text{where} \quad (10a)$$

$$P_\cap(\beta) := P - \alpha \beta P \mathbf{f} \mathbf{f}^T P, \quad (10b)$$

$$\mathbf{c}_\cap(\beta) := \mathbf{c} + \alpha \beta \delta P \mathbf{f}, \quad (10c)$$

$$\varsigma_\cap(\beta) := \varsigma + \alpha \beta \left(\frac{\gamma^2}{1-\beta} - \delta^2 \right), \quad (10c)$$

$$\text{else if } \underline{y} = \bar{y} = -\rho, \text{ then } \mathbf{x} = \mathbf{c} - \varsigma^{\frac{1}{2}} (\mathbf{f}^T P \mathbf{f})^{-\frac{1}{2}} P \mathbf{f}; \quad (10d)$$

$$\text{else if } \underline{y} = \bar{y} = \bar{\rho}, \text{ then } \mathbf{x} = \mathbf{c} + \varsigma^{\frac{1}{2}} (\mathbf{f}^T P \mathbf{f})^{-\frac{1}{2}} P \mathbf{f}; \quad (10e)$$

$$\text{else if } -\rho < \underline{y} = \bar{y} < \bar{\rho}, \mathbf{x} \in \mathcal{E}(\mathbf{c}_\cap(1), (\varsigma - \alpha \delta^2) P_\cap(1)) \quad (10f)$$

$$\text{otherwise (if } \underline{y} = \bar{y} = \bar{\rho} = -\rho), \mathbf{x} \in \mathcal{E}(\mathbf{c}, \varsigma P); \quad (10g)$$

where

$$\alpha := (\mathbf{f}^T P \mathbf{f})^{-1}, \quad (10h)$$

$$\delta := \frac{1}{2}(\bar{\nu} + \nu) - \mathbf{f}^T \mathbf{c} = \frac{1}{2}(\bar{\nu} + \nu - \bar{\rho} + \rho), \quad (10i)$$

$$\gamma := \frac{1}{2}(\bar{\nu} - \nu), \quad (10j)$$

$$\bar{\nu} := \min(\bar{y}, \bar{\rho}), \quad \nu := \max(\underline{y}, -\rho), \quad (10k)$$

$$\rho := \sqrt{\varsigma \mathbf{f}^T P \mathbf{f}} - \mathbf{c}^T \mathbf{f}, \quad \bar{\rho} := \sqrt{\varsigma \mathbf{f}^T P \mathbf{f}} + \mathbf{c}^T \mathbf{f}. \quad (10l)$$

Proof. *cf.* Appendix B.2 and B.6 in [5] (Thms 4.2 and 4.4). \square

A. Optimal value of the parameter β

In the case where the ellipsoid's usual volume can be zero, the optimal value for the weighting parameter β , intervening in (10a)-(10c) and minimizing the pseudo-volume of the ellipsoid $\mathcal{E}_\cap(\beta)$, is derived below.

³If \mathcal{H} contains \mathcal{E} , meaning that $\mathcal{H} \subset \mathcal{R}(P)$, this hyperplane is redundant and is not carrying any useful information (*cf.* Thm 4.4 of [3]). Now \mathcal{H} can be parallel to \mathcal{E} , only if the constraint carried by this hyperplane is faulty, which is assumed to be impossible here.

Theorem 4.2: If $\mathcal{E}_\cap(\beta)$ given by (10) of Thm 4.1, for which $q := \text{rank}(P) \geq 1$, then

$$\beta^* := \arg \min_{\beta \in]0, 1[} \text{spv}(\mathcal{E}_\cap(\beta)) = \begin{cases} \frac{-a_1 - \sqrt{a_1^2 - 4a_0 a_2}}{2a_2}, & \text{if } a_0 < 0, \\ 0, & \text{otherwise;} \end{cases}$$

$$\text{where } a_0 := q\alpha(\gamma^2 - \delta^2) - \varsigma, \quad (11a)$$

$$a_1 := (2q+1)\alpha\delta^2 + \varsigma - \gamma^2\alpha, \quad (11b)$$

$$a_2 := -(q+1)\alpha\delta^2, \quad (11c)$$

Furthermore, if $a_0 < 0$, then $\text{spv}(\mathcal{E}_\cap(\beta^*)) < \text{spv}(\mathcal{E})$. (11d)

Proof. *cf.* Appendix B.4 in [5] (Thm 4.3.2). \square

B. The output update algorithm

The state estimation algorithm's measurement update stage is established in the following.

Theorem 4.3: Let \mathbf{x}_k satisfy (1) and (2). $\forall k \in \mathbb{N}^*$, $\mathcal{E}_k := \mathcal{E}(\hat{\mathbf{x}}_k, \varsigma_k P_k)$, that contains the set \mathcal{S}_k (*cf.* (9)), has the smallest pseudo-volume possible, if and only if

$$\forall k \notin \mathcal{K} \text{ (i.e. } p_k = 0), \quad \mathcal{E}_k := \mathcal{E}_{k/k-1} \quad \text{and} \quad (12a)$$

$$\forall k \in \mathcal{K}, \quad \hat{\mathbf{x}}_k := \xi_p, P_k := \Pi_p, \varsigma_k := \sigma_p, q_k := \kappa_p, \quad (12b)$$

$$\xi_i := \xi_{i-1} + \alpha_i \beta_i \delta_i \Pi_{i-1} \mathbf{f}_{k_i}, \quad \xi_0 := \hat{\mathbf{x}}_{k/k-1}, \quad (12c)$$

$$\Pi_i := \Pi_{i-1} - \alpha_i \beta_i \Pi_{i-1} \mathbf{f}_{k_i} \mathbf{f}_{k_i}^T \Pi_{i-1}, \quad \Pi_0 := P_{k/k-1}, \quad (12d)$$

$$\sigma_i := \begin{cases} \sigma_{i-1} - \alpha_i \beta_i^2 \delta_i^2, & \text{if } \nu_i = \bar{\nu}_i \wedge -\rho_i \neq \bar{\rho}_i, \\ \sigma_{i-1} + \alpha_i \beta_i \left(\frac{\gamma_i^2}{1-\beta_i} - \delta_i^2 \right), & \text{otherwise;} \end{cases} \quad (12e)$$

$$\kappa_i := \begin{cases} \kappa_{i-1} - 1, & \text{if } \nu_i = \bar{\nu}_i \wedge -\rho_i \neq \bar{\rho}_i \wedge \alpha_i \neq 0 \\ \kappa_{i-1}, & \text{otherwise} \quad (\kappa_i := \text{rank}(\Pi_i)); \end{cases} \quad (12f)$$

$i \in \{1, \dots, p_k\}$; $\sigma_0 := \varsigma_{k-1}$, $\kappa_0 := q_{k/k-1}$ given in (8e), where $\hat{\mathbf{x}}_{k/k-1}$ and $P_{k/k-1} := Q_m$ are computed according to Thms 3.5, 3.6 and where

$$\alpha_i := \begin{cases} (\mathbf{f}_{k_i}^T \Pi_{i-1} \mathbf{f}_{k_i})^{-1}, & \text{if } \Pi_{i-1} \mathbf{f}_{k_i} \neq \mathbf{0}_n, \\ 0, & \text{otherwise;} \end{cases} \quad (12g)$$

$$\beta_i := \begin{cases} 1, & \text{if } \nu_i = \bar{\nu}_i \wedge -\rho_i \neq \bar{\rho}_i, \\ \beta^*, & \text{else if } -\rho_i < \nu_i \vee \bar{\nu}_i < \bar{\rho}_i, \\ 0, & \text{otherwise;} \end{cases} \quad (12h)$$

β^* given by Thm 4.2 with $\alpha := \alpha_i$, $\gamma := \gamma_i$, $\delta := \delta_i$, $\varsigma := \sigma_{i-1}$,

$$\delta_i := \frac{1}{2}(\bar{\nu}_i + \nu_i) - \mathbf{f}_{k_i}^T \xi_{i-1}, \quad \gamma_i := \frac{1}{2}(\bar{\nu}_i - \nu_i), \quad (12i)$$

$$\bar{\rho}_i := \sqrt{\frac{\sigma_{i-1}}{\alpha_i}} + \mathbf{f}_{k_i}^T \xi_{i-1}, \quad \rho_i := \sqrt{\frac{\sigma_{i-1}}{\alpha_i}} - \mathbf{f}_{k_i}^T \xi_{i-1}, \quad (12j)$$

$$\bar{\nu}_i := \min(\bar{y}_{k_i}, \bar{\rho}_i) \text{ and } \nu_i := \max(y_{k_i}, -\rho_i). \quad (12k)$$

Proof. *cf.* Appendix B.7 in [5] (Thm 4.5). \square

Thm 4.3 is reproduced in Algorithm 2, where \mathcal{E}_k is computed from $\mathcal{E}_{k/k-1}$ (Algo. 1).

Remark 4.1: If one of the two hyperplanes that bound the strip containing the state vector and representing the measurement $i \in \mathcal{D}_k$ is outside the ellipsoid $\mathcal{E}_{k_{i-1}} := \mathcal{E}(\xi_{i-1}, \varsigma_{k_{i-1}} \Pi_{i-1})$, the strip reduction at eq. (12k) (line 7 of Algo. 2) significantly reduces the size of the resulting ellipsoid, according to [7].

Remark 4.2: The computational complexity of this algorithm is $O(n2)$. All of the operations are, in fact, simple sums and products. Because they were optimized in this way, they are suitable for systems with a high dimensional state vector (big n), a large number of measurements (big p_k)

and a large number of unknown bounded inputs (big m_k). In order to perform redundant vector and matrix operations only once, the intermediate variables α , θ , η and φ were added. Additionally, rather than multiplying potentially high dimensional vectors, in (12g), (12j), (12i) and (12d)-(12e), scalar arithmetic is used, at lines 5, 6, 8 and 24 *resp.* It should be noticed that $\mathbf{f}_{k_i}^T \xi_{i-1} = \frac{1}{2}(\bar{\rho}_i - \rho_i)$ allowed to reformulate δ_i and ρ_i .

Remark 4.3: In the case where $\mathcal{H}_k \neq \emptyset$, the matrix Π_i loses rank with each intersecting hyperplane (equality constraint), for $i \in \mathcal{H}_k$, thusly entailing the progressive flattening of the ellipsoid \mathcal{E}_{k_i} . Depending on the rank of the matrix R_k , the rank of $P_{k+1/k}$ can be restored at the time-update phase. The value of the rank of \mathcal{E}_k 's shape matrix is needed at the prediction phase. Therefore, this parameter is tracked through a simple relation, (8c), during the time update and is decremented, by (12f), at each hyperplane intersection, during the observation update. Hence, provided that $\text{rank}(A_0 P_0 A_0^T)$ is given, there is no need to recalculate this rank at each step i .

Remark 4.4: Setting either $\alpha_i = 0$ or $\beta_i = 0$ causes $\mathcal{E}_{k_{i-1}}$ to freeze, meaning that the corresponding measurements $\mathbf{f}_{k_i}, \mathcal{V}_i, \bar{\mathcal{V}}_i$ do not bring any useful information. This also allows to consider the scenario in which the measurement $\{\mathbf{f}_{k_i}, \mathcal{V}_i, \bar{\mathcal{V}}_i\}$ is aberrant, preventing the update of the ellipsoid $\mathcal{E}_{k_{i-1}}$.

V. ESTIMATION ALGORITHM AND STABILITY ANALYSIS

A. The overall state estimation algorithm

The prediction stage given by Thms 3.5 and 3.6 and the correction stage, given by Thm 4.3, are concatenated to form the whole state estimation algorithm, presented in Algo. 3, where N is the number of samples (time steps k). Please note the normalization carried out on the line 5: P_k would thereby represent the shape matrix of the ellipsoid \mathcal{E}_k up to a constant factor ς_0^{-1} . ς_0 is used, instead of ς_k and ς_{k-1} , as inputs to Algo. 1 and 2 *resp.* ς_k is only used to track its evolution.

B. Stability analysis

In this section, we'll show the boundedness of the pseudo-volume of \mathcal{E}_k .

Theorem 5.1: Consider the system (1) subject to (2) and its state estimation algorithm given by Thms 3.5, 3.6 and 4.3.

$$F_{\mathcal{C}} := \begin{cases} [\mathbf{f}_{k_i}]_{i \in \mathcal{C}_k} \in \mathbb{R}^{n \times p_{\mathcal{C}}}, & \forall k \in \mathcal{K}_{\mathcal{C}}, \\ 0_{n, p_{\mathcal{C}}}, & \forall k \notin \mathcal{K}_{\mathcal{C}} \end{cases} \quad (13a)$$

where $\mathcal{K}_{\mathcal{C}} = \{k \in \mathbb{N}^* | p_{\mathcal{C}} \neq 0\}$ and $p_{\mathcal{C}} := \text{Card}(\mathcal{C}_k)$, *cf.* (9). If A_k is invertible and the pairs $\{A_k, F_{\mathcal{C}}^T\}$ and $\{A_k, R_k\}$ are *sporadically observable* and uniformly controllable *resp.*⁴, then

1. the pseudo-volume of the ellipsoid $\mathcal{E}_k := \mathcal{E}(\hat{\mathbf{x}}_k, \varsigma_k P_k)$ is bounded, *i.e.*, $\frac{1}{v_k} \text{spv}(\mathcal{E}_k)$ is nonincreasing and $\text{spv}(\mathcal{E}_k) \leq v_k \text{spv}(\mathcal{E}_0)$, where $v_0 = 1$ and

$$v_k := \prod_{j=0}^{k-1} \left| \Lambda_j P_j P_j^\dagger \right|_{\dagger}^2 \left| \Phi_j^\dagger \Phi_j + (\Phi_j^\dagger + I_n - \Phi_j^\dagger \Phi_j) W_j \right|_{\dagger};$$

$$\Phi_j := \Lambda_j P_j \Lambda_j^T; \Lambda_j := \prod_{i=1}^m \sqrt{1 + \mu_i A_j}, \mu_i \in]0, 1[;$$

⁴*cf.* Definitions A.1 and A.3 in [8].

Algorithm 2 Minimal pseudo-volume corrected ellipsoid

Input: $\mathbf{x}, P, \varsigma, q, \mathbf{f}_1, \dots, \mathbf{f}_p, \bar{\mathbf{y}}, \mathbf{y}, p$

Output: $\mathbf{x}, P, \varsigma, q$

```

1: if  $p \neq 0$  then
2:   for  $i = 1, \dots, p$  do
3:      $\varphi := P \mathbf{f}_i; \theta := \mathbf{f}_i^T \varphi; \eta := (\varsigma \theta)^{\frac{1}{2}}; \{\text{new variables}\}$ 
4:     if  $\theta \neq 0$  then
5:        $\alpha := \theta^{-1}; \{\text{cf. (12g)}\};$ 
6:        $\bar{\rho} := \eta + \mathbf{f}_i^T \mathbf{x}; \rho := 2\eta - \bar{\rho}; \{\text{cf. (12j)}\};$ 
7:        $\bar{\mathbf{y}} := \min(\bar{\mathbf{y}}_i, \bar{\rho}); \mathbf{y} := \max(\mathbf{y}_i, -\rho); \{\text{cf. (12k)}\};$ 
8:        $\delta := \frac{1}{2}(\bar{\mathbf{y}} + \mathbf{y} - \bar{\rho} + \rho); \gamma := \frac{1}{2}(\bar{\mathbf{y}} - \mathbf{y}); \{\text{cf. (12i)}\};$ 
9:       if  $\mathbf{y} = \bar{\mathbf{y}}$  and  $-\rho \neq \bar{\rho}$  then
10:         $\beta = 1;$ 
11:         $q \leftarrow q - 1$ 
12:       else if  $-\rho < \mathbf{y}$  or  $\bar{\mathbf{y}} < \bar{\rho}$  then
13:         $a_0 := q\alpha(\gamma^2 - \delta^2) - \varsigma; \{\text{cf. (11a)}\};$ 
14:        if  $a_0 \geq 0$  then
15:           $\beta := 0;$ 
16:        else
17:           $a_1 := (2q + 1)\alpha\delta^2 + \varsigma - \gamma^2\alpha; \{\text{cf. (11b)}\}$ 
18:           $a_2 := -(q + 1)\alpha\delta^2; \{\text{cf. (11c)}\};$ 
19:           $\beta := \frac{-a_1 + \sqrt{a_1^2 - 4a_0a_2}}{2a_2};$ 
20:        end if
21:       else
22:         $\beta = 0;$ 
23:       end if
24:        $P \leftarrow P - \alpha\beta\varphi\varphi^T; \mathbf{x} \leftarrow \mathbf{x} + \alpha\beta\delta\varphi;$ 
25:        $\varsigma \leftarrow \varsigma - \alpha\beta^2\delta^2; \{\text{cf. (12d)-(12e)}\};$ 
26:     end if
27:   end for

```

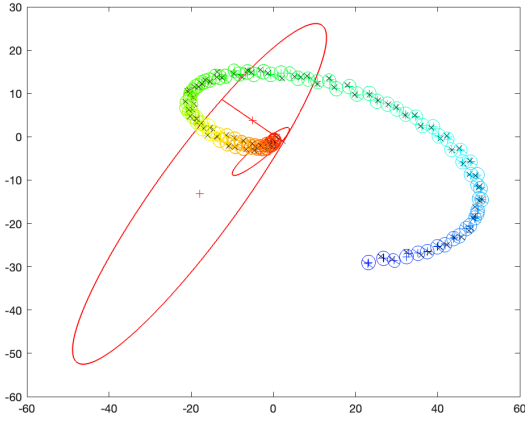
$$W_j := \frac{1}{\varsigma_j} R_j \text{Diag}\left(\frac{\chi_i}{\mu_i}\right)_{i=1}^m R_j^T, \chi_i = \prod_{j=i}^m (1 + \mu_j). \quad (13b)$$

2. Furthermore, if $\|A_k\| \leq 1$ (where $\|A\| := \sup_{\mathbf{x} \neq 0} \frac{\|A\mathbf{x}\|}{\|\mathbf{x}\|}$) and $R_k = 0_{n,m}, \forall k \in \mathbb{N}$, then $\text{spv}(\mathcal{E}_k)$ is nonincreasing.

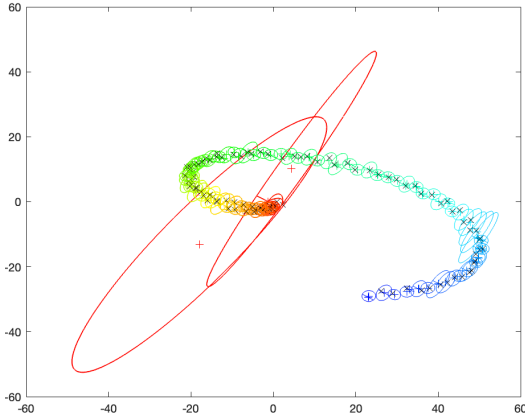
Proof. *cf.* Appendix C.3 in [5] (Thm 5.4). \square

VI. NUMERICAL SIMULATIONS

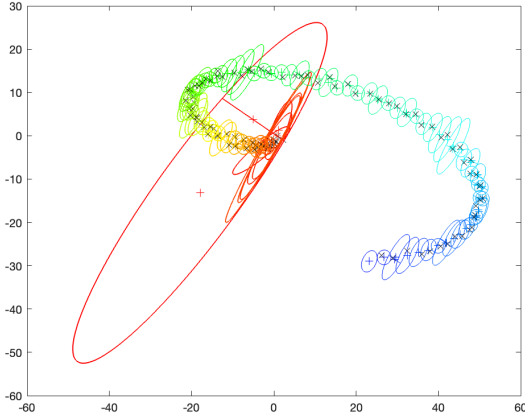
For the sake of graphic illustration, the presented algorithm is applied to a second order stable randomly generated system with coil-shaped input for $k = 0, \dots, 100$. The components of all the matrices intervening in the model (1)-(2) are constant normally distributed pseudorandom numbers. Two measurements are available: one with upper and/or lower bound (of either strip or halfspace type) and the second representing an equality constraint (hyperplane), randomly and sporadically generated. The figures 1a – 1d show the evolution of the ellipsoid \mathcal{E}_k when the measurements are taken at all 100, 90, 50 and only 20 randomly chosen time-steps among 100, *resp.* \mathcal{E}_0 is red and \mathcal{E}_{100} is blue. $\hat{\mathbf{x}}_k$ and \mathbf{x}_k are represented by '+' and 'x' *resp.* It is plain to see how the ellipsoid shrinks when the measurements are available and how it expands in their absence, under the effect of the process noise contained in a zonotope that is added to the ellipsoid at each time step.



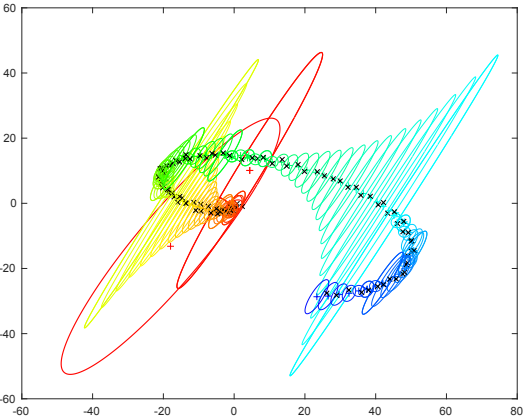
a Measurements at all time steps



b Measurements at 90 steps/100



c Measurements at 50 steps/100



d Measurements at 20 steps/100

Algorithm 3 Minimal pseudo-volume ellipsoid $\mathcal{E}(\hat{\mathbf{x}}_k, \varsigma_k P_k)$

Input: $\hat{\mathbf{x}}_0, \varsigma_0, P_0, N, n$ (size of $\hat{\mathbf{x}}_0$);

Output: $\hat{\mathbf{x}}_k, \varsigma_k, P_k, k \in \{1, \dots, N\}$.

- 1: **for** $k = 0, 1, \dots, N - 1$ **do**
 - 2: Algorithm 1 (**Input:** $\hat{\mathbf{x}}_k, P_k, \varsigma_0, q_k, A_k, B_k, R_k, \boldsymbol{\tau}_k, m_k$; **Output** $\hat{\mathbf{x}}_{k+1/k}, P_{k+1/k}, q_{k+1/k}$)
 - 3: $k \leftarrow k + 1$
 - 4: Algorithm 2 (**Input:** $\hat{\mathbf{x}}_{k/k-1}, P_{k/k-1}, \varsigma_0, q_{k/k-1}, F_k, \tilde{\mathbf{y}}_k, \mathbf{y}_k, p_k$; **Output:** $\hat{\mathbf{x}}_k, P_k, \varsigma_k, q_k$)
 - 5: $P_k \leftarrow \frac{\varsigma_k}{\varsigma_0} P_k$; $\varsigma_k \leftarrow \frac{\varsigma_0 \varsigma_k}{\varsigma_{k-1}}$;
 - 6: **end for**
-

VII. CONCLUSION

An ellipsoidal state bounding approach was proposed for discrete-time LTV models with sporadic measurements corrupted by additive unknown process and measurement disturbances and subject to equality constraints on the state vector. The presence of equality constraints inducing the rank loss and the noninvertibility of the state bounding ellipsoid shape matrix makes a difference from the existing algorithms. Special attention was given to numerical stability and computational simplicity in terms of time and memory. The computational complexity of the proposed algorithm is $\mathcal{O}(n^3)$, where each time step k comprises only one $(n \times n)$ pseudoinverse, two $(n \times n)$ matrix products, and some n -vector products, in addition to scalar arithmetics.

Furthermore, the proposed method—which was presented in an optimized, detailed, and straightforward turnkey pseudocode—can be implemented without the use of complicated tools, convex optimization techniques, heavy libraries or specific expertise. Some convergence conditions were formulated despite the sporadic character of the measurements and the state constraints manifesting themselves occasionally, not necessarily simultaneously and not at all time steps.

REFERENCES

- [1] D. Simon, “Kalman filtering with state constraints: A survey of linear and nonlinear algorithms,” *Control Theory and Applications, IET*, vol. 4, pp. 1303 – 1318, 09 2010.
- [2] L. E. Andersson, L. Imsland, E. F. Brekke, and F. Scibilia, “On kalman filtering with linear state equality constraints,” *Automatica*, vol. 101, pp. 467 – 470, 2019.
- [3] Y. Becis-Aubry, “Ellipsoidal constrained state estimation in presence of bounded disturbances,” in *European Control Conference*, June 2021.
- [4] L. Ros, A. Sabater, and F. Thomas, “An ellipsoidal calculus based on propagation and fusion,” *IEEE transactions on systems, man, and cybernetics. Part B, Cybernetics : a publication of the IEEE Systems, Man, and Cybernetics Society*, vol. 32 4, pp. 430–42, 2002.
- [5] Y. Becis-Aubry, “Bounded-error constrained state estimation in presence of sporadic measurements,” <https://arxiv.org/abs/2202.13900>, 2022.
- [6] C. D. Meyer, Jr., “Generalized inversion of modified matrices,” *SIAM Journal on Applied Mathematics*, vol. 24, no. 3, pp. 315–323, 1973.
- [7] G. Belforte, B. Bona, and V. Cerone, “Parameter Estimation Algorithm for a Set-Membership Description of Uncertainty,” *Automatica*, vol. 26, no. 5, pp. 887–898, Sept. 1990.
- [8] Y. Becis-Aubry, “Ellipsoidal constrained state estimation in presence of bounded disturbances,” 2020. [Online]. Available: <https://arxiv.org/abs/2012.03267>